Wind and Structures, *Vol. 22, No. 6 (2016) 635-662*
DOI: http://dx.doi.org/10.12989/was.2016.22.6.635

Comparative study of control strategies for the induction generators in wind energy conversion system

D. Giribabu[*1], Maloy Das[1a] and Amit Kumar[2b]

[1]*NIT Kurukshetra, Department of Electrical Engineering, Kurukshetra-136119, India*
[2]*NIT Kurukshetra, School of Renewable Energy, Kurukshetra-136119, India*

(Received January 21, 2016, Revised April 14, 2016, Accepted April 20, 2016)

Abstract. This paper deals with the comparison of different control strategies for the Induction generators in wind energy conversion system. Mainly, two types of induction machines, Self excited induction generator (SEIG) and doubly Fed Induction generators (DFIG) are studied. The different control strategies for SEIG and DFIG are compared. For SEIG, Electronic load Controller mechanism, Static Compensator based voltage regulator are studied. For DFIG the main control strategy namely vector control, direct torque control and direct power control are implemented. Apart from these control strategies for both SEIG and DFIG to improve the performance, the ANFIS based controller is introduced in both STATCOM and DTC methods. These control methods are simulated using MATLAB/SIMULINK and performances are analyzed and compared.

Keywords: Self excited induction generator (SEIG); doubly fed induction generator (DFIG); Electronic load Controller (ELC); Static Compensator (STATCOM); Adaptive Neuro Fuzzy Interface System (ANFIS); Vector control (VC); Direct Torque control (DTC) and Direct power control (DPC)

1. Introduction

Now a day's the non-conventional sources of energy are being exhausts. This is the right time to focus on conventional sources of energy like solar, wind, tidal/wave, biomass and small hydro energy. In remote location, converting the electrical energy from these resources can be very cheaper and easier. Among this sources solar and wind energy are in front of the race. But like wind energy, solar can't provide electricity in continuously. So wind energy is more preferable. The total installed capacity of wind energy has been increasing all over the world in the recent years. In 2015 total global wind power installed was 63 GW. The new global total at the end of 2015 was 432.9 GW as per Global Wind Report (2015). To convert the wind energy to electrical energy various types of generators like induction generator, permanent magnet synchronous generator (PMSG) and doubly fed induction generator can be used.

Induction generator is preferred over PMSG due to robustness and easy maintenance. Induction

∗Corresponding author, Assistant Professor, E-mail: dgiribabu208@gmail.com
[a] M.Tech. Student, E-mail: maloy674@gmail.com
[b] M.Tech. Student, E-mail: amit.yuvraaj09@gmail.com

http://www.techno-press.org/?journal=was&subpage=8 ISSN: 1226-6116 (Print), 1598-6225 (Online)

generators are of two types, self-excited induction generator (SEIG) and doubly fed induction generator (DFIG). According to Smith (1996), Rajakaruna and Bonert (1993), Alghuwainem (1999), SEIGs are preferred in remote areas for low power rating. The SEIGs can be used to generate constant voltage and frequency if the electrical load is maintained constant at its terminals. Any decrease in load may accelerate the machine speed and raise the voltage and frequency levels to dangerously high values to affect other connected loads, and also when the SEIGs are driven by constant power prime mover the frequency of the generated voltage is almost constant, but the voltage regulation is poor.

Several methods are proposed to overcome the limitations which are introduced in Singh *et al.*(2003), Makky *et al.* (1997), Bonert and Hoops (1989), Henderson (1998), Suarez and Bortolotto (1999), Bhim Singh *et al.* (2005), Bhim Singh *et al.* (2006), Bhim Singh *et al.* (2014). The methods reported in B. Singh *et al.*(2003), Makky *et al.* (1997), Bonert and Hoops (1989), Henderson (1998) have employed ELC's such as phase controlled thyristor based load controller, controlled rectifier feeding dump loads, switched resistor based controller, uncontrolled rectifier based load controller etc. Among these first three are controlled by firing angle. Due to a delay in firing angle, it demands reactive power loading and injects harmonics into the system causing unbalancing source current and source voltage. Further it requires driver circuits which are complicated. The voltage regulation methods are discussed in Suarez and Bortolotto (1999), Bhim Singh *et al.* (2005), Bhim Singh *et al.* (2006) are based on long shunt and short shunt compensation method which employing only passive elements. These passive elements are not capable of regulating the terminal voltage when the load changes. Thus STATCOM based controller is used in Bhim Singh *et al.* (2014) which feeding single phase loads and the conventional PI controller is used.

Now a day's doubly fed induction generators (DFIG) are one of the most widely used technology for wind power generation due to certain advantages like, wide speed range, smooth active and reactive power regulation, flexibility and robustness. DFIG have windings on both stator and rotor. Through both the windings there is a significant amount of active power transfer between shaft and electrical system. However DFIG based wind energy conversion system have some challenges like power quality issues (Nunes *et al*. 2004), stability of grid (E. Tremblay *et al.* 2006), and low voltage ride through capability.

Several methods are proposed to overcome the limitations which are introduced in Tremblay *et al.* (2011), Pingle *et al.* (2015), Zarean and Kazemi (2012), Habetler *et al.* (1992), Alnasir and Almarhoon (2012), Zhi and Xu (2007), Datta and Ranganathan (2001), Noguchi *et al.* (1996), Tremblay *et al.* (2009), Guo *et al.* (2008). In Tremblay *et al.* (2011), Pingle *et al.* (2015) vector control methods for controlling active and reactive power have been studied. Although steady state performance of VC is excellent and it gives quick dynamic response, it depends on the machine parameters accuracy and much tuning effort is required to ensure the system stability over the entire operation range, the DTC of DFIG has been studied in literature Zarean and Kazemi (2012), Habetler *et al.* (1992), Alnasir and Almarhoon (2012). In DTC method the desired stator voltage vector, stator flux position and the error signs of both torque and flux are directly estimated to restrict the torque and flux errors within their respective hysteresis bands. In Zarean and Kazemi (2012) direct torque control method is discussed based on the rotor power factor by keeping it equal to one and rotor voltage vectors is obtained by using look-up table. Direct torque control using space vector modulation is studied in Habetler *et al.* (1992). Design and modeling of DTC is studied in Alnasir and Almarhoon (2012). Direct power control strategy (DPC) for enhanced control and operation of DFIG has been studied in Zhi and Xu (2007), Datta and Ranganathan

(2001), Noguchi *et al.* (1996), Tremblay *et al.* (2009), Guo *et al.* (2008) and has been proved to have several advantages over vector control and direct torque control method. In Zhi and Xu (2007) the transient performance of DFIG has been improved using DPC. Dependency on machine model and computational complexity is less in DPC. For DTC, in most of the literatures PI controller has been used for estimating the reference torque. Despite the merits of simple structure and quick response, the implementation of the DTC-PI controller requires fine tuning and in case of parameter variation the switching frequency of switching devices becomes unpredictable. Also there is problem of overshoot and ripples. Various methods have been proposed to eliminate these drawbacks, such as fuzzy logic control, neural network (NN) control, and adaptive neuro-fuzzy control. In Chitra Venugopal (2010), Moghadasia *et al.* (2011), Mechernene *et al.* (2010), Sudhakar and Vijaya Kumar (2012), Aware *et al.* (2000), Jacomini *et al.* (2014), Kusagur *et al.* (2010) the ANFIS controller for controlling induction machines has been studied. The ANFIS controller is more accurate and its yield better performance as compared to conventional PI controller.

In this paper to improve the performance of SEIG and DFIG ANFIS controller is implemented. Various control strategies for SEIG and DFIG are studied and compared. SEIG is used for constant speed operation. In variable speed generation DFIG is more dominantly used because it allows the turbine for variable speed operation.

2. Mathematical modeling of induction generator

The dynamic model of the three-phase induction generator is developed by using a stationary d-q-axes reference frame (Suarez and Bortolotto 1999, Bhim Singh *et al.* 2005) and the relevant volt-current equations are

$$[v] = [R][i] + [L]p[i] + w_g[G][i] \tag{1}$$

The current derivative can be expressed as

$$p[i] = [L]^{-1}\{[v] - [R][i] - w_g[G][i]\} \tag{2}$$

Developed electromagnetic torque is,

$$T_e = \left(\frac{3P}{4}\right) L_m (i_{qs} i_{dr} - i_{ds} i_{qr}) \tag{3}$$

Torque balance equation is

$$T_{shaft} = T_e + J\left(\frac{2}{P}\right) p w_g \tag{4}$$

The magnetizing current equation is

$$I_m = \frac{\{(i_{ds}+i_{dr})^2 + (i_{qs}+i_{qr})^2\}^{1/2}}{\sqrt{2}} \tag{5}$$

The magnetizing inductance (L_m) is calculated from magnetizing characteristic as,

$$L_m = a + bI_m + cI_m{}^2 + dI_m{}^3 \tag{6}$$

Where

$$[v] = [v_{ds} \quad v_{qs} \quad v_{dr} \ v_{qr}]^T$$

$$[i] = [i_{ds} \ i_{qs} i_{dr} i_{qr}]^T$$

$$[R] = \text{diagonal}[R_s \ R_s R_r R_r]$$

$$[L] = \begin{bmatrix} L_{ss} & 0 & L_m & 0 \\ 0 & L_{ss} & 0 & L_m \\ L_m & 0 & L_{rr} & 0 \\ 0 & L_m & 0 & L_{rr} \end{bmatrix}$$

$$[G] = \begin{bmatrix} 0 & 0 & 0 & 0 \\ 0 & 0 & 0 & 0 \\ 0 & -L_m & 0 & L_{rr} \\ L_m & 0 & L_{rr} & 0 \end{bmatrix}$$

Where

$$L_{ss} = L_s + L_m \ ,$$

$$L_{rr} = L_r + L_m$$

[R]= SEIG resistance,
[L]= SEIG inductance,
[G]= speed inductance,
P = number of poles,
T_{shaft}= input torque,
a,b,c,d= coefficient of magnetizing curve,
$(a = 0.1437 b = 0.0014 \ c = -0.0012 \ d = 0.00005)$

Here, subscript d,q refers to the d and q axis components, s and r refers to the stator and rotor and m is magnetizing component.

The DFIG model in d-q reference frame can be represented as (7-10). (Tremblay *et al.* 2011)

$$v_{ds} = R_s i_{ds} + p\varphi_{ds} - w_s\varphi_{qs} \tag{7}$$

$$v_{qs} = R_s i_{qs} + p\varphi_{qs} + w_s\varphi_{ds} \tag{8}$$

$$v_{dr} = R_r i_{dr} + p\varphi_{dr} - (w_s - w_r)\varphi_{qr} \tag{9}$$

$$v_{qr} = R_r i_{qr} + p\varphi_{qr} - (w_s - w_r)\varphi_{dr} \tag{10}$$

In case of SEIG, V_{dr} and V_{qr} becomes zero.

The stator and rotor flux linkage equations are given as

$$\varphi_{ds} = L_s i_{ds} + L_m i_{dr} \tag{11}$$

$$\varphi_{qs} = L_s i_{qs} + L_m i_{qr} \tag{12}$$

$$\varphi_{dr} = L_r i_{dr} + L_m i_{ds} \tag{13}$$

$$\varphi_{qr} = L_r i_{qr} + L_m i_{qs} \tag{14}$$

Where,

$$L_s = L_{ls} + L_m \tag{15}$$
$$L_r = L_{lr} + L_m \tag{16}$$

L_{ls} And L_{lr} are stator and rotor leakage inductance respectively and L_m is the mutual inductance.

3. SEIG with electronıc load controller

3.1 System configuration

The schematic diagram of SEIG-ELC & its control circuit is shown in Fig. 1 and 2 respectively. The SEIG-ELC system consists of a three phase SEIG driven by a constant power prime mover. The Excitation capacitors are connected at the terminals of SEIG. The ELC consists of a uncontrolled rectifier in series with a chopper and dump load. The chopper circuit consists of an insulated gate bipolar transistor (IGBT). By controlling this IGBT the dump load will come into action when there is change in the load at SEIG terminals. The output terminal voltage of SEIG is sensed with a voltage sensor and is rectified by diode bridge rectifier (DBR), which is compared with reference voltage to obtain the gate signal of chopper circuit through a PI controller. Since the input power of the SEIG is constant, the output power of the SEIG is need to be constant at varying consumer loads. Thus, through this ELC the power in surplus of the consumer load is dumped in the dump load and the SEIG feeds two loads in parallel such that the load power is constant.

The performance of SEIG using ELC for a three phase 7.5-kW 400-V four pole Star connected self-exited induction generator are shown in Fig. 3. Here the load is resistive, reactive, and capacitive. The detailed data are given in Appendix I. The Fig. 4 shows the voltage buildup of SEIG. A capacitor bank of 500 μF/phase is connected across the SEIG terminal as excitation capacitance. It can be observed that the voltage build up process starts at 0.2s. The ELC system is simulated at different load conditions.

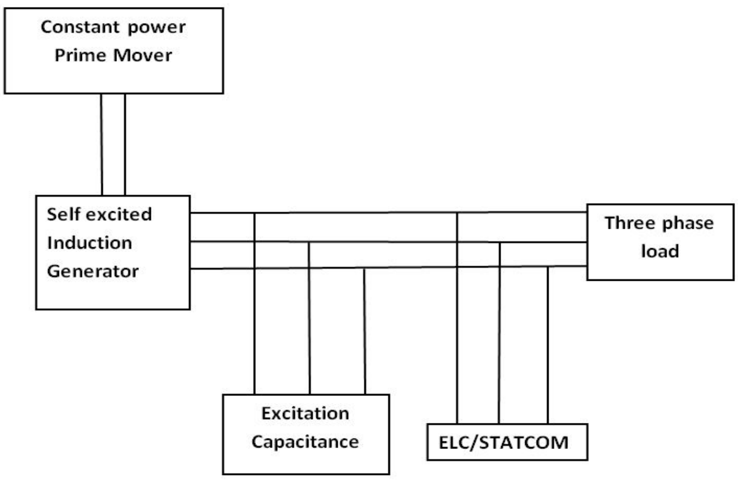

Fig. 1 Schematic diagram of three-phase SEIG-ELC/STATCOM

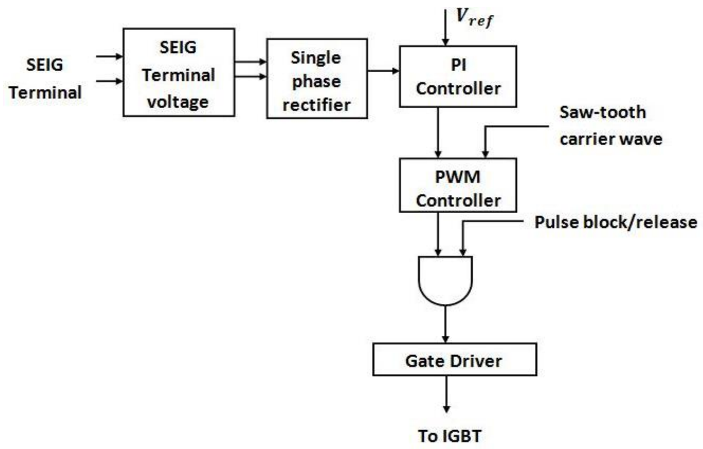

Fig. 2 Control circuit for SEIG-ELC system

Load varied from 1000 Ω to 2000 Ω resistive load, RLC load consisting R=200 Ω, L=100 mH, C=10 µF, RL load consisting R=100 Ω, L=100 mH etc. It can be observed that the load voltage remains constant with varying load but the voltage and current signals are not purely sinusoidal. When any change is occurs in the consumer load the ELC with the dump load act like a non-linear load. The rectifier output has ripple which should be filtered. Therefore a filtering capacitor is connected at output terminal of rectifier a filtering capacitor of 4000µF is used to smooth the dc voltage. Here the dump load is 120 Ω.

The power in surplus of the consumer load is dumped in the resistance through the ELC. Thus the SEIG feeds two loads in parallel such that the total load remains constant. But as the ELC acts like a non-linear load it injects harmonic currents into the SEIG. THD of order of 15.8% in SEIG voltage is observed in Fig. 4.

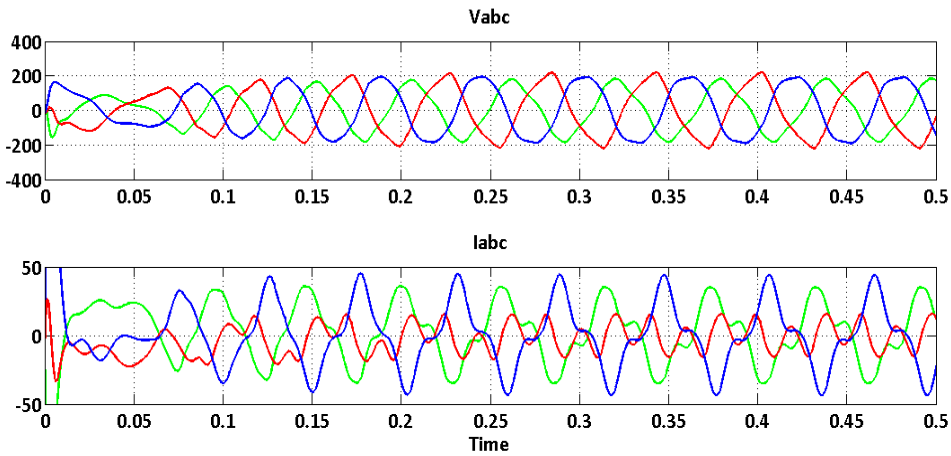

Fig. 3 voltage and current waveform of SEIG-ELC with RLC load (R=200 Ω, L=100 mH, C=10 µF)

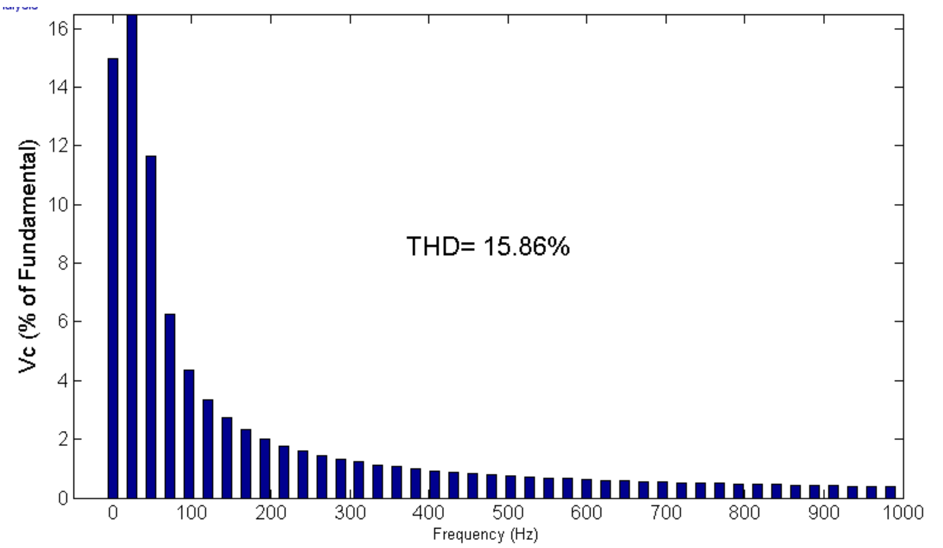

Fig. 4 Harmonic Spectrum of SEIG-ELC voltage

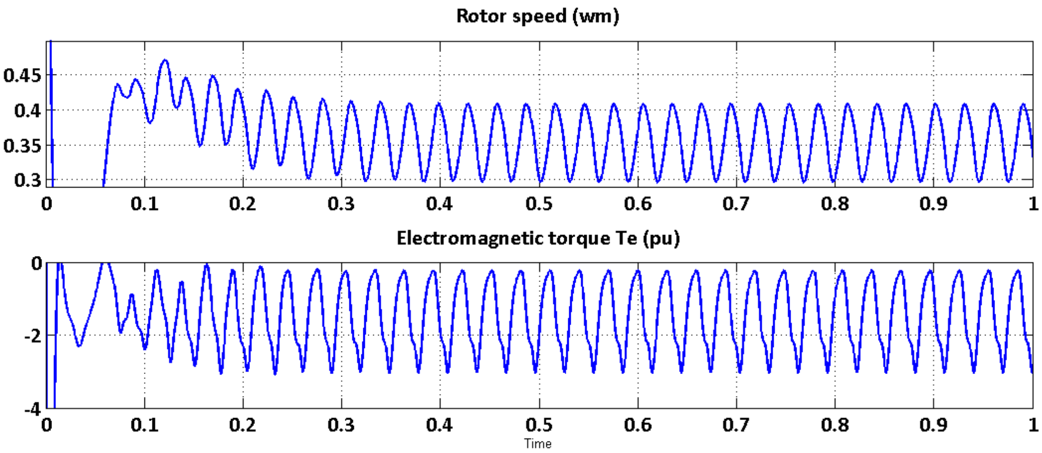

Fig. 5 SEIG-STATCOM Rotor speed and Electromagnetic torque

The rotor speed and electromagnetic torque is also fluctuating which is need to be improved.

4. SEIG with STATCOM based voltage regulator

4.1 System configuration

The ELC in the schematic of SEIG can be replaced with STATCOM. Here, load controller is

STATCOM based voltage controller. The STACOM is a three phase IGBT based current controlled voltage source inverter connected with a DC bus capacitor. The SEIG terminal voltage is controlled by controlling the source current. This algorithm is based on the transformation of source currents to synchronous rotating d-q frame. Fig. 6 shows the block diagram of the controlling algorithm. Here the three phase load currents are sensed and three phase quantities are transforming into two phase α-β quantities. The source voltages V_a, V_b, V_c are processed through phase-locked loop (PLL) to generate unit voltage template. Then the source current signals transformed to d-q reference frame. The d-q-axis load currents component contains two parts namely fundamental component ($\overline{I_{ld}}$) and oscillatory component ($\widetilde{I_{ld}}$) as

$$I_{ld} = \overline{I_{ld}} + \widetilde{I_{ld}} \tag{17}$$

$$I_{lq} = \overline{I_{lq}} + \widetilde{I_{lq}} \tag{18}$$

The oscillatory part is due to the non-linearity of the loads. Even if the load is linear it still contains some oscillatory component. By eliminating the oscillatory component in the load current the power quality can be improved. Hence, these signals are passed through a low pass filter to eliminate the oscillatory parts. The dc-bus capacitor voltage (V_{dc}) of the STATCOM is sensed and compared with the reference signal (V_{dcref}) and the voltageerror is fed to a PI controller. The output of the PI controller is the active power component of current (I_{loss}) that to meet the losses of STATCOM. The source should supply the loss component of the STATCOM with filtered equivalent d-axis component of the load. Thus resultant d-axis component current can be expressed as

$$I_D = \frac{\overline{I_{ld}} + I_{loss}}{3} \tag{19}$$

For regulating the system voltage the STATCOM has to inject reactive power component of current to meet the reactive power demands. This can be estimated by sensing the phase voltages at the SEIG terminals. The SEIG terminal voltages (V_t) are sensed and compared with the reference voltage (V_{tref}) which is assured to maintain the SEIG terminal voltage. Here the amplitude of sensed SEIG voltage at SEIG terminal is expressed as

$$V_t = \sqrt{\frac{2}{3}\left(v_a^2 + v_b^2 + v_c^2\right)} \tag{20}$$

The error signal V_t and reference voltage signal (V_{tref}) is fed to the PI controller. The output of PI controller(I_{pi}) with the filtered q-axis component of current makes the resultant q-axis component of current which should be supplied by the source to maintain the terminal voltage at a reference voltage.

The resultant q-axis component of current is expressed as

$$I_Q = \frac{\overline{I_{lq}} + I_{pi}}{3} \tag{21}$$

Using these d-axis and q-axis component of current the α-β axis components of the reference current can be estimated. From this α-β frame the three phase reference source currents. Now the sensed source currents are compared with this reference source currents and the error signal is fed to the PWM pulse generator for switching the IGBTs of the STATCOM.

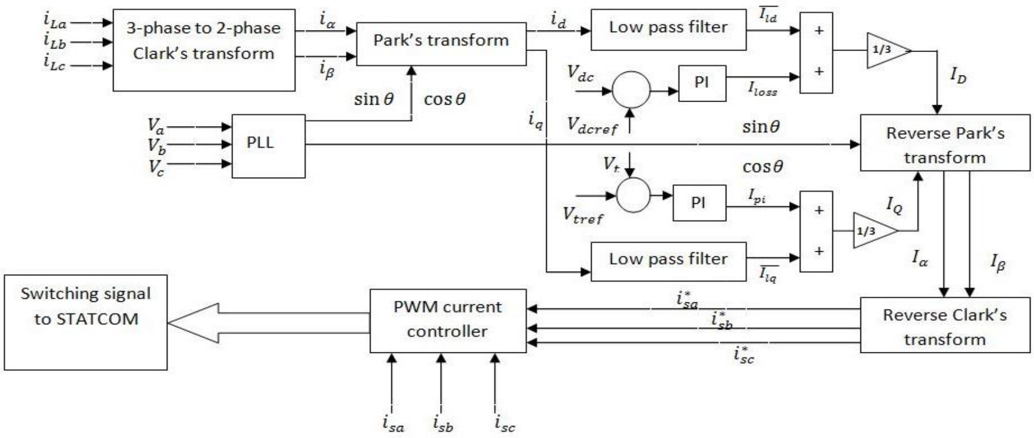

Fig. 6 Control circuit for SEIG-STATCOM system

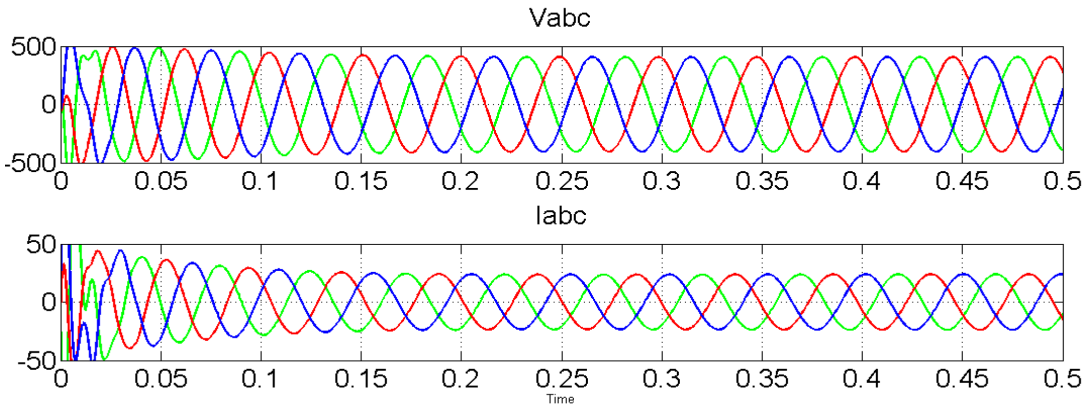

Fig. 7 SEIG-STATCOM voltage and current

Fig. 7 shows the performance of SEIG with STATCOM based voltage regulator. Here the system feeding three phase linear and non-linear load. In case of STATCOM controller the current at any instant can be divided into reactive power and active power components. The reactive power component is regulating the terminal voltage and active power component delivered the active power. For constant SEIG current if reactive power component decreases, active power component increased and vice versa. The simulation study is carried for similar load condition as on the previous case. In this case the generation of voltage template using PLL plays an important role in the calculation of reference source currents. In the Fig. 7 the SEIG terminal voltages are constant at 400V which is the rated voltage and the currents are balanced which clearly displays the harmonic mitigation capability of STATCOM as compared to ELC. The voltage harmonic spectrum is shown in Fig.8. The rotor speed and electromagnetic torque fluctuation is also become less as compared to ELC but more improvement is required. The speed and torque graph is shown in Fig. 9.

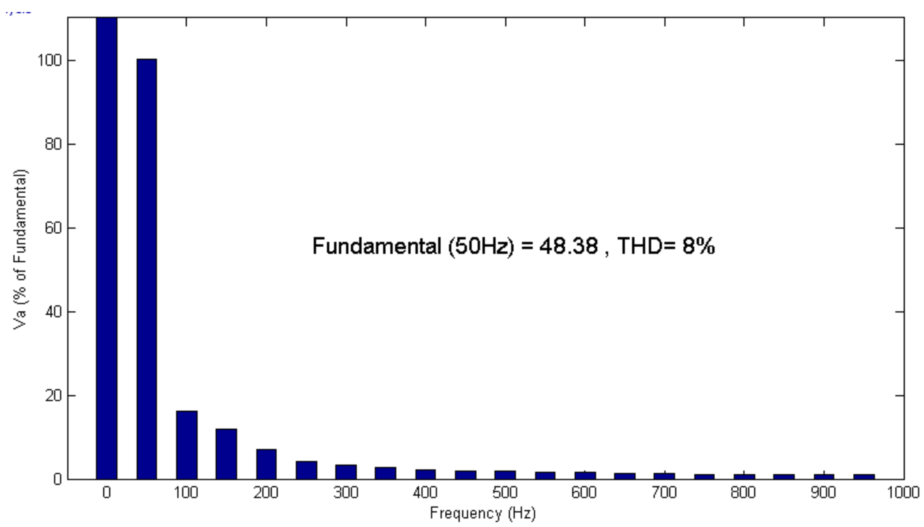

Fig. 8 Harmonic Spectrum of SEIG-STATCOM voltage

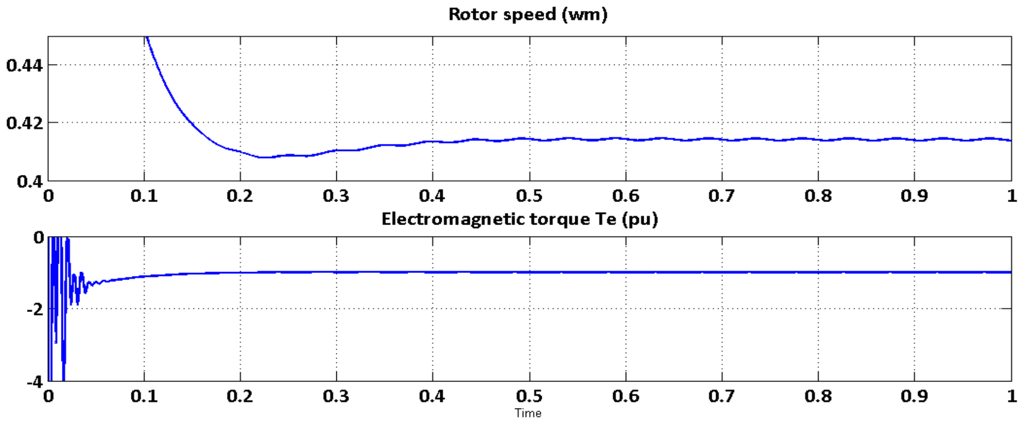

Fig. 9 SEIG-STATCOM Rotor speed and Electromagnetic torque

5. DFIG in wind energy conversion systems

Doubly fed induction generator is mainly used in wind energy applications. DFIG have windings on both stator and rotor. Through both the windings there is a significant amount of active power transfer between shaft and electrical system. The block diagram of a grid connected DFIG based wind energy conversion system is shown in Fig. 10. Stator winding is connected directly to the grid, whereas rotor winding is connected to grid via slip rings and back to back voltage source converter (VSC). Converters are used to control grid and rotor current. Thus the active and reactive power fed from stator to the grid is controlled irrespective of wind speed. The two converters are connected through a dc-link capacitor which reduces the ripples in the dc-link voltage.

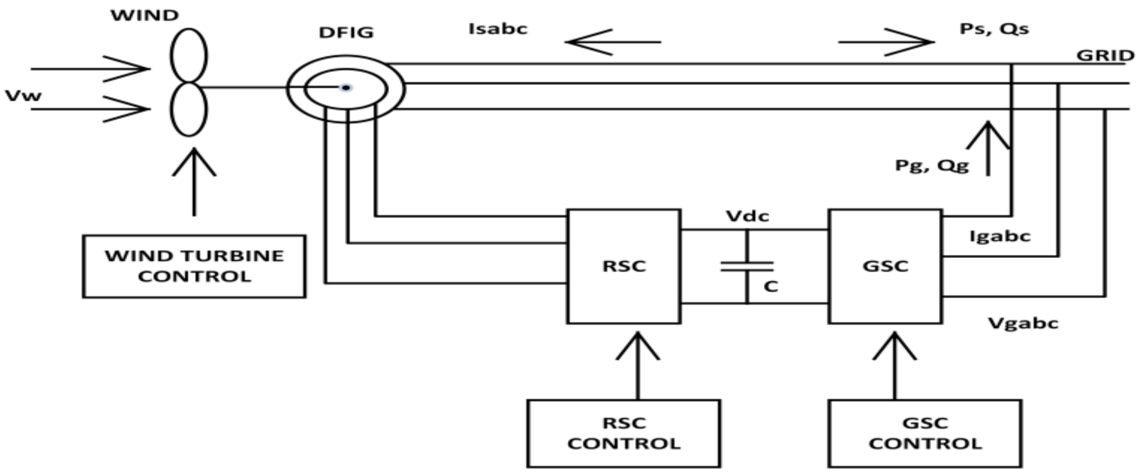

Fig. 10 Grid connected DFIG -based WECS

In DFIG the rotor is basically wound rotor whose winding is 2 to 3 times the stator winding. Thus the Rotor voltage is higher and current is lower, which reduces the cost of the converter.

DFIG is controlled by Vector control (VC), Direct torque control (DTC), and Direct power control (DPC).

6. Vector control of the DFIG

6.1 Basic principle of VC

DFIG can be controlled by controlling rotor side converter and grid side converter. VC can be used for both. The objective of the Vector control for RSC is to regulate stator active power Ps and reactive power Qs independently. The overall RSC control scheme using Vector control is shown in Fig. 11.To describe the control scheme, the general park's model of DFIG is used. Using the conventions in static stator oriented reference frame, voltage vector equations are written as

$$V_s = R_s i_s + \frac{d\varphi_s}{dt} \tag{22}$$

$$V_r = R_r i_r + \frac{d\varphi_r}{dt} - jw\varphi_r \tag{23}$$

$$\varphi_s = L_s i_s + L_m i_r \tag{24}$$

$$\varphi_r = L_m i_s + L_r i_r \tag{25}$$

The vector control scheme consists of two series of two PI controllers. The active and reactive power error signals are given to the two different PI controller which gives direct rotor current I_{rd}^*, and quadrature current I_{rq}^* respectively. These two signals are compared with the generator currents, I_{rd} and I_{rq} and the error signal is given to the other two PI controllers. The outputof these controllers is rotor voltage V_{rd} and V_{rq} respectively.

From rotor voltage equations

$$V_{rd} = R_r i_{rd} + \sigma L_r \frac{di_{rd}}{dt} \quad (26)$$

$$V_{rq} = R_r i_{rq} + \sigma L_r \frac{di_{rq}}{dt} \quad (27)$$

Where, σ is the leakage factor defined as,

$$\sigma = 1 - \frac{L_m^2}{L_s L_r} \quad (28)$$

To ensure good tracking of rotor d-q axis currents, compensation terms are added to V_{rd} and V_{rq}

$$V_{rd}^* = V_{rd} - w_{slip}\sigma L_r i_{rq} \quad (29)$$

$$V_{rq}^* = V_{rq} + w_{slip}(\sigma L_r I_{rd} + L_m i_{rd}) \quad (30)$$

The voltage signals are given to the PWM generator which gives pulses to the rotor side converter.

The proposed vector control of DFIG in wind power application is verified using MATLAB/SIMULINK software. The parameters used are listed in table III. For a step change in wind speed from 10 m/s to 12 m/s, the variation in active power rotor speed of the generator is shown in Fig. 12 shows active power shoots up to 0.8 pu and rotor speed shoots above synchronous speed and settles at 1.4 pu. The reference and generated current characteristics is also shown.

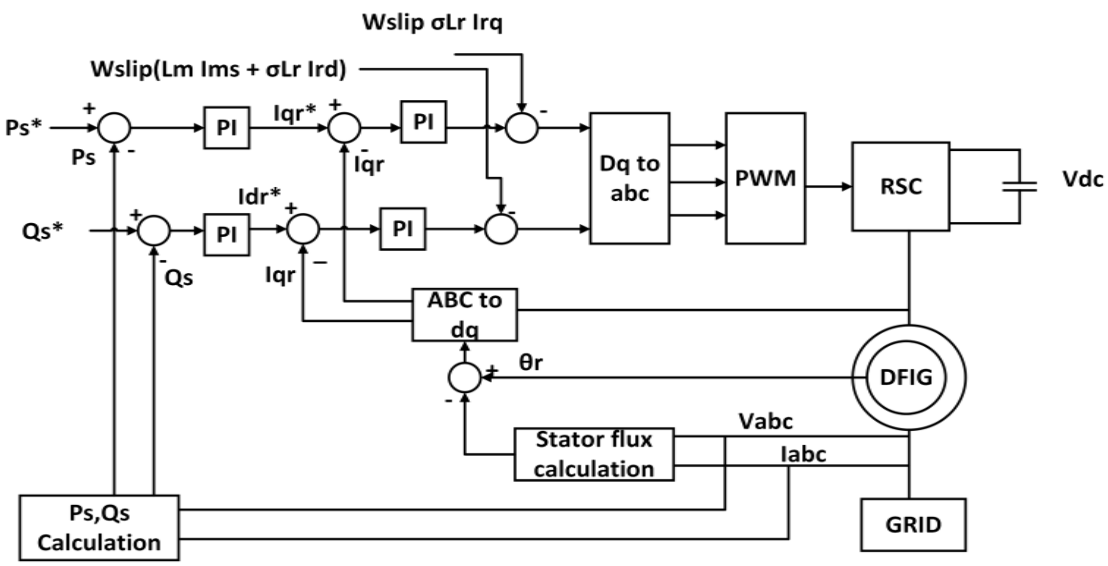

Fig. 11 Vector control structure for DFIG

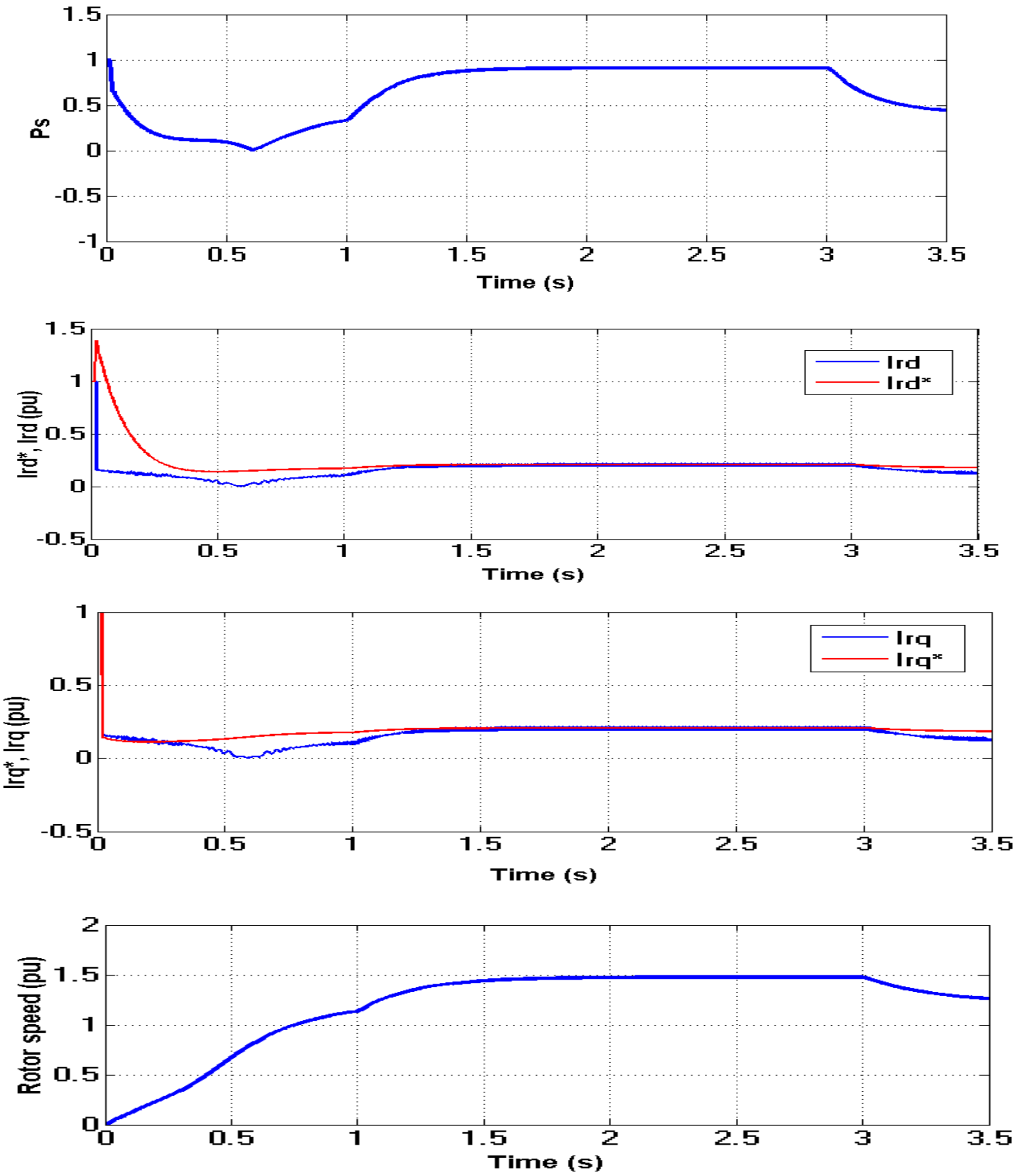

Fig. 12 Simulation result of vector control of DFIG

7. Direct torque control of the DFIG

DTC technique was first proposed in 1986 by Takahashi and Noguchi. DTC strategy for doubly-fed induction generator (DFIG) provides a simple control structure and high efficiency. It has much simpler configuration compared to VC. In this method rotor power factor is maintained at unity and a switching table is obtained which gives rotor voltage vector. Inverter output voltage space vector directly influences the stator flux. By selecting appropriate voltage vector desired locus of stator flux is obtained. Torque changes due to changing of stator flux.

7.1 Principal of DTC

The torque of induction machine is given as

$$\mathrm{T_e} = -\frac{3}{2}\mathrm{n_p}\frac{\mathrm{L_m}}{\mathrm{L_s L_r - L_m^2}}|\varphi_s||\varphi_r|\sin\theta \tag{31}$$

Where, n_p is the number of pole pairs, L_s is the stator inductance, L_r is the rotor inductance, L_m is the mutual inductance between stator and rotor. Φ_s and φ_r are the stator and rotor flux respectively and θ is the phase angle difference between them. Stator flux is given by

$$\varphi_s = \int(\mathrm{v_s} - \mathrm{i_s R_s})\,\mathrm{dt} \tag{32}$$

Neglecting stator resistance drop

$$\varphi_s = \int(\mathrm{v_s})\,\mathrm{dt}\ \text{or} \frac{\mathrm{d}\varphi_s}{\mathrm{dt}} = \mathrm{v_s} \tag{33}$$

Change in stator flux directly depends upon output voltage space vector. Rotor time constant of induction machine is very large therefore rotor flux changes slowly compared to stator flux and assumed to be constant. When forward active voltage space vectors are applied, the stator flux linkage moves away from the rotor flux linkage vector. This increases torque angle and hence torque is increased. When zero or backward active voltage space vectors are applied, the stator flux linkage moves toward the rotor flux linkage vector. This decreases torque angle and hence torque is reduced.

7.2 DTC system of DFIG based WECS

DTC strategy for DFIG based wind energy conversion system is shown in Fig. 13. DTC technique consists of torque and stator flux estimators, two hysteresis controllers and a switching table.

The voltage across the stator is given by following expressions.

$$\mathrm{v_{ds}} = \mathrm{R_s i_{ds}} + \frac{\mathrm{d}\varphi_{\mathrm{ds}}}{\mathrm{dt}} \tag{34}$$

$$\mathrm{v_{qs}} = \mathrm{R_s i_{qs}} + \frac{\mathrm{d}\varphi_{\mathrm{qs}}}{\mathrm{dt}} \tag{35}$$

Stator direct and quadrature flux can be written from Eqs. (34) and (35) as following

$$\varphi_{\mathrm{ds}} = \int(\mathrm{v_{ds}} - \mathrm{R_s i_{ds}})\mathrm{dt} \tag{36}$$

$$\varphi_{\mathrm{qs}} = \int(\mathrm{v_{qs}} - \mathrm{R_s i_{qs}})\mathrm{dt} \tag{37}$$

$$\varphi_s = \varphi_{\mathrm{ds}} + \mathrm{j}\,\varphi_{\mathrm{qs}} \tag{38}$$

$$\mathrm{T_e} = \frac{3}{2}\mathrm{P}\left(\mathrm{i_{qs}}\varphi_{\mathrm{ds}} - \mathrm{i_{ds}}\varphi_{\mathrm{qs}}\right) \tag{39}$$

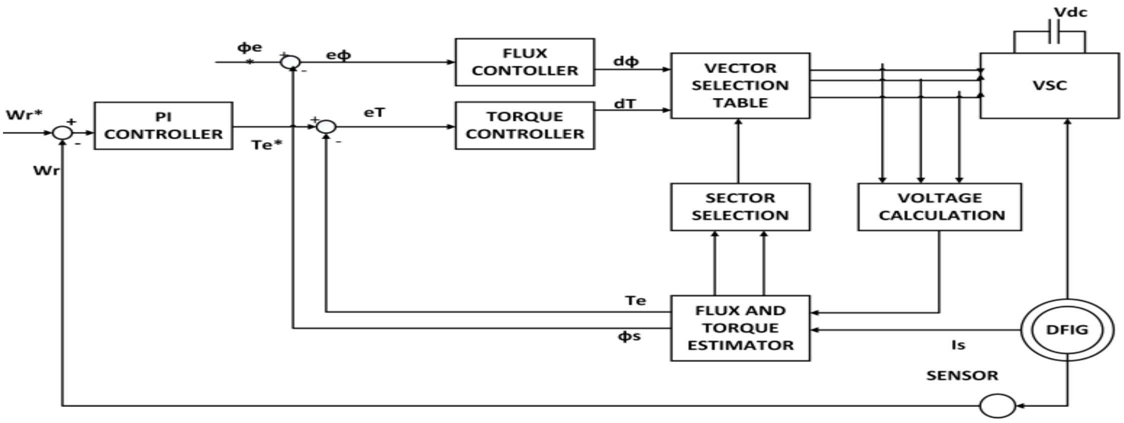

Fig. 13 DTC system of DFIG

The estimated torque and flux are controlled by hysteresis controller. For flux two level hysteresis controllers is used and for torque three levels hysteresis controller is used. These controllers provides their error status d_{φ}andd_{Te}. These output signals are defined as

$$d_{\phi} = 1 \text{ for } e_{\phi} > H_{\phi} \tag{40a}$$

$$d_{\phi} = 0 \text{ for } e_{\phi} < H_{\phi} \tag{40b}$$

$$d_{Te} = 1 \text{ for } e_{Te} > H_{Te} \tag{40c}$$

$$d_{Te} = 0 \text{ for } e_{Te} = 0 \tag{40d}$$

$$d_{Te} = -1 \text{ for } e_{Te} < H_{Te} \tag{40e}$$

In classical DTC method the plane is divided in six sectors. These sectors together with d_{φ} and d_{Te} selects appropriate voltage vector from switching table. These voltage vectors controls magnitude and angle of stator flux. The voltage vector and six 60° sectors associated with them are shown in Fig. 14.

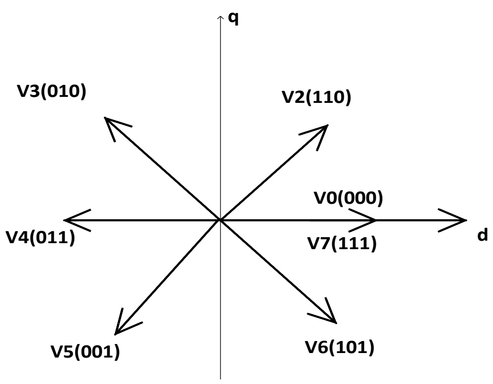

Fig. 14 Space voltage vector

There are six none zero and two zero space vectors. If the stator flux space vector lies in K_{th} sector, where k=1, 2…6, its magnitude can be increased by using the voltage vectors, k, k+1, k-1.Rest three voltage vector reduces its magnitude. For example if stator flux space vector lies in sector 1 then its magnitude is increased by applying voltage vectors V1, V2 and V6 and is decreased by applying V3, V4, V5.For torque, if increase/decrease in torque is required then voltage vector which are ahead/behind of stator flux space vector in the direction of rotation are applied. Zero vectors are applied for no change in torque. So by combining the three factors- sector, torque change and flux change a voltage vector look-up table is designed. The switching table is shown in Table 1.

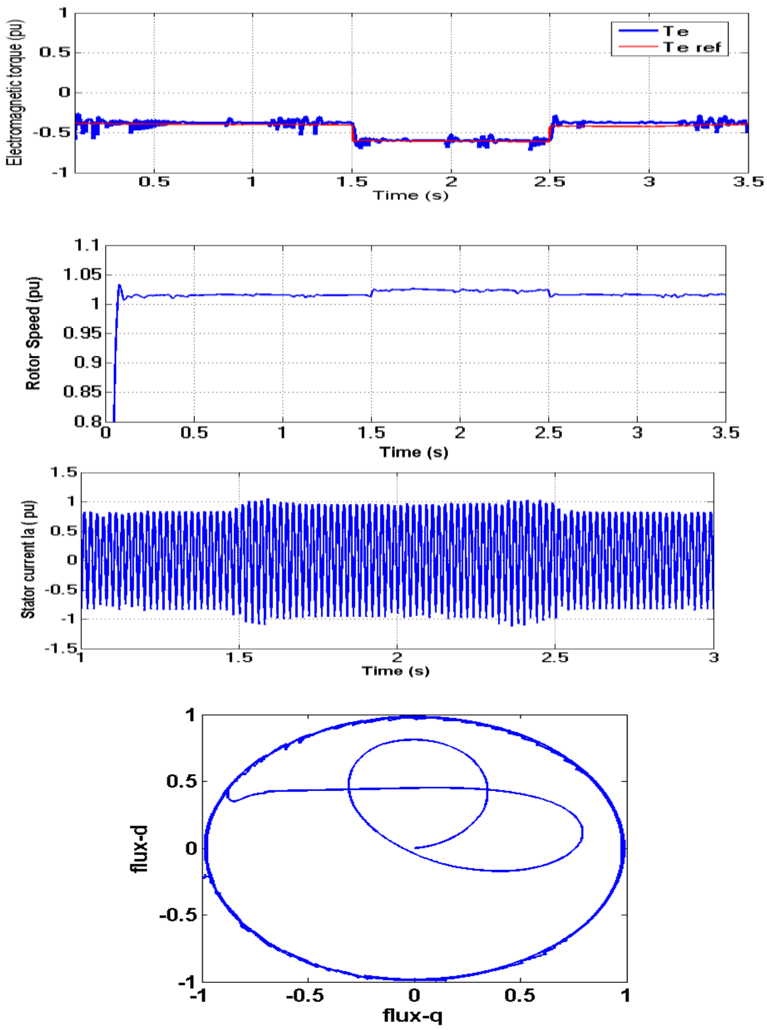

Fig. 15 Simulation results for DTC of DFIG

Table 1 DTC optimal vector selection

Error status		Sector no.					
Φs	Te	1	2	3	4	5	6
0	1	110	010	011	001	101	100
	0	111	000	111	000	111	000
	-1	011	001	101	100	110	010
1	1	100	110	010	011	001	101
	0	000	111	000	111	000	111
	-1	001	101	100	110	010	011

The simulation study is carried using MATLAB/SIMULINK software to prove that the validate DTC of the DFIG in wind power application. The parameters used are listed in Appendix II. The following results are obtained for a condition step increase in wind speed from 10 m/s to 12 m/s at 1.5 s and a step decrease from 12 m/s to 10 m/s at 2.5 s. These results show the better performance for electromagnetic torque, rotor speed, stator current and rotor flux characteristics.

8. Direct power control of the DFIG

8.1 DPC theoretical background

The DPC basic principle is almost similar to the DTC. DPC is also dependent on the geometrical relationship between stator and rotor fluxes and the rotor flux can be fully controlled by controlling the RSC. However in DPC, instead of directly controlling the torque and flux, we control the effect of these parameters over stator active and reactive power. The DPC strategy is simpler and robust when compared to VC and DTC. The main features of DPC include independence from machine parameters and reduced number of electrical magnitudes to be measured, and there is no need for reference frame transformations in DPC (Zhi and Xu 2007).

Instantaneous stator active and reactive powers in d-q frame are determined by following equations

$$P_s = \frac{3}{2}\left(v_{\beta s} i_{\beta s} + v_{\alpha s} i_{\alpha s}\right) \tag{41}$$

$$Q_s = \frac{3}{2}\left(v_{\beta s} i_{\alpha s} + v_{\alpha s} i_{\beta s}\right) \tag{42}$$

The estimated active and reactive powers are controlled by hysteresis controller. Two three-level hysteresis comparators are used to generate the respective active and reactive power states Sp and Sq. The voltage vectors and sectors are similar to the DTC discussed above. Based on the above analysis, the optimal switching table is arranged and it is shown in Table 2.Fig.16 shows the schematic diagram of the proposed DPC strategy.

As shown in Fig. 16, the three-phase ac stator voltages and currents are measured and transformed into the stationary α–β reference frame. The active and reactive powers are calculated and the stator flux is then estimated. The rotor speed issued to transform the stator flux from the stator frame to the rotor frame. The calculated active and reactive powers are compared to their reference values and error signals Sp and Sq are generated. The two active and reactive power states are then fed to the optimal switching table together with the calculated stator flux position to obtain the appropriate switching states. Finally, the optimal switching states are fed to the rotor side converter to provide the control required to reduce the power errors.

The direct power control (DPC) of DFIG in wind power application is verified using MATLAB/SIMULINK software. The parameters used are listed in Appendix II. The following results are obtained for a step change in wind speed from 8 m/s to 12 m/s at 0.5 s. Fig.17 show active power, reactive power stator voltage and current characteristics.

9. Induction generator performance improvement using ANFIS controller

9.1 ANFIS concept

Adaptive neuro-fuzzy control is a very powerful technique which basically uses the concept of both fuzzy controller and artificial neural network. ANNs are a collection of intelligent algorithms which are used for control, time series prediction and identification purposes of various parameter of induction machine. The fuzzy based controller has good capability to be interpreted and they work on the basis of previous random experiences. Combining fuzzy and ANN forms an intelligent system which has good learning capabilities, good interpretation and prior knowledge. They form rule base to give control signal. ANFIS controller ensures selecting a proper membership function and in turn selecting the correct rule base.

Table 2 DPC optimal vector selection

Error status		Sector no.					
Sq	Sp	1	2	3	4	5	6
1	1	101	100	110	010	011	001
	0	100	110	010	011	001	101
	-1	110	010	011	001	101	100
0	1	001	101	100	110	010	011
	0	000	111	000	111	000	111
	-1	010	011	001	101	100	110
-1	1	001	101	100	110	010	011
	0	011	001	101	100	110	010
	-1	010	011	001	101	100	110

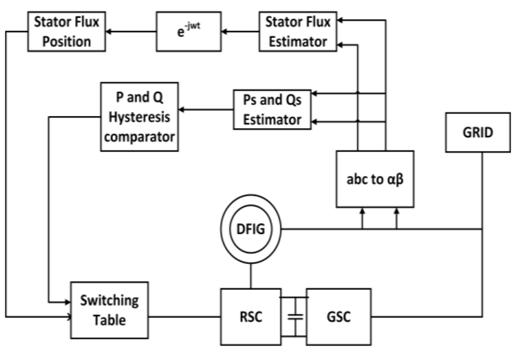

Fig. 16 DPC scheme of DFIG based WECS

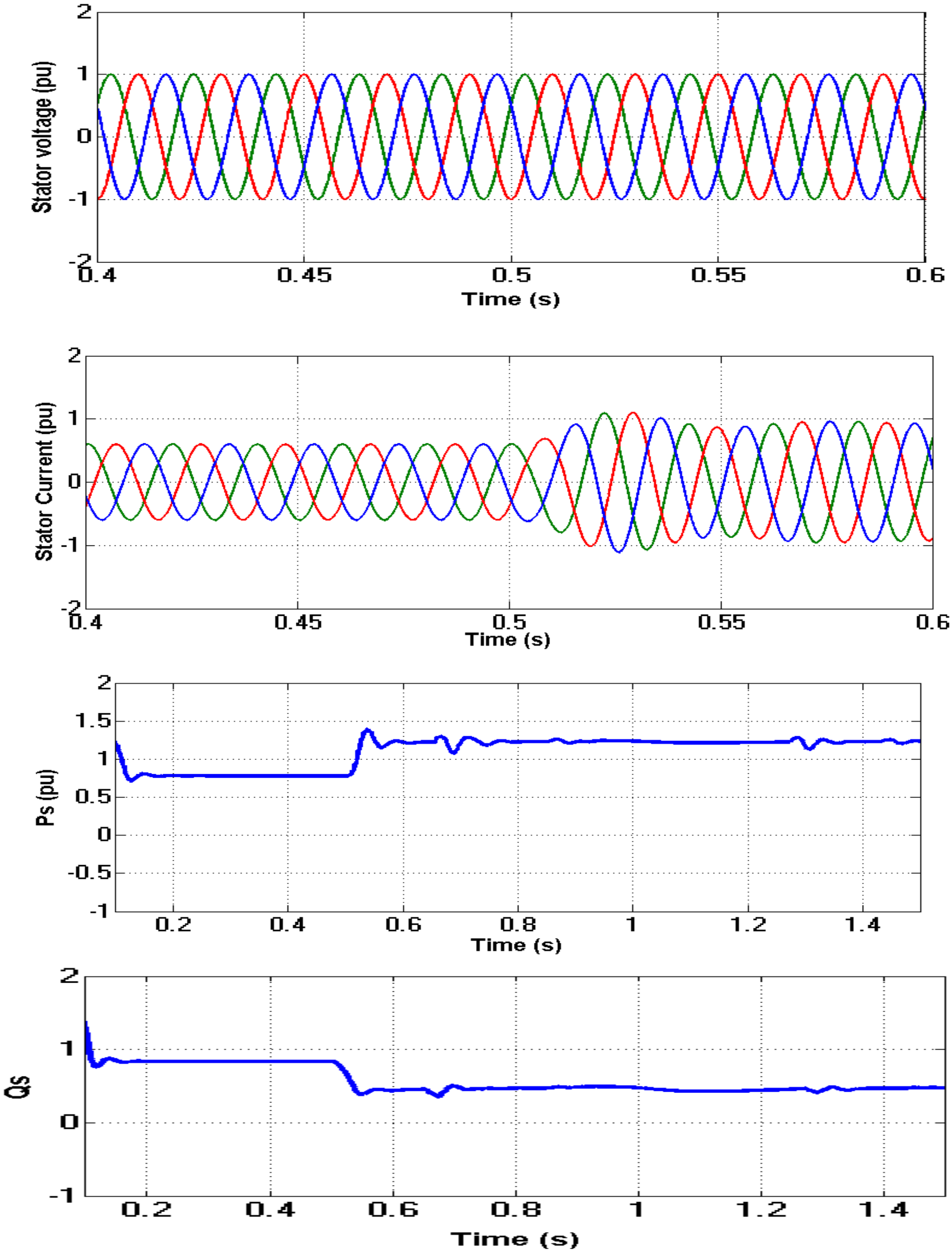

Fig. 17 Simulation results for DPC of DFIG

9.2 ANFIS model

The ANFIS model architecture supports the TL-FLC method. The rules are in linguistic form so interpretation and analysis of intermediate results are possible. During training rules can be modified manually. The first requirement of ANFIS training is a training data set consisting of desired input and output pairs of system to be modelled. The design parameters required for any ANFIS controller are viz., Number of data pairs, Training data set & checking data sets, Fuzzy inference systems for training, Number of epochs to be chosen to start the training, Learning results to be verified after mentioning the step size (Sudhakar and Vijaya 2012).

ANFIS control structure is presented here as follows (Jacomani *et al*. 2014). The general ANFIS structure consists of a set of units arranged into five connected network layers.

Layer 1: In this layer all the nodes present consists of the membership function, or input variables. Input variables are supplied to the next layer.

Layer 2: Minimum value of weights for the two input is chosen by this node. It represents the fuzzy set of each variables received from layer 1.

Layer 3: All the nodes in this layer calculate the weight, which is normalized. Fuzzy rules are matched in this layer.

Layer 4: This is the defuzzification layer which provides output by the help of rules. Normalization is performed by each neuron in this layer.

Layer 5: This is the output layer which sums all the incoming signals and fuzzy classification result is transformed to binary.

9.3 ANFIS controller design

ANFIS controller is designed for controlling various parameters like, torque, speed, flux, voltage and current of the induction machine. The block diagram of the control scheme is shown in Fig.18. The basic structure of the ANFIS controller consists of 4 important parts, viz., fuzzification, knowledge base, neural network and the de-fuzzification blocks (Sudhakar and Vijaya 2012). The inputs to the ANFIS controller are the error and change in the error represented by following equations:

$$\mathrm{e(k)} = \mathrm{W_{ref}} - \mathrm{W_r} \tag{43}$$

$$\Delta\mathrm{e(k)} = \mathrm{e(k)} - \mathrm{e(k-1)} \tag{44}$$

Where$\mathrm{W_{ref}}$ is the reference speed,$\mathrm{W_r}$ is the actual rotor speed, e(k) is the error and $\Delta\mathrm{e(k)}$ is the change in error.

In the fuzzification unit crisp data is converted into linguistic variables, which is given as inputs to the rule based block. The rule based block consists of set of 49 rules which are written on the basis of previous knowledge (Kusagur *et al*. 2010). The output of rule base is given to the neural network block. Neural network is trained using back propagation algorithm for selecting proper set of rule base. The output of the NN unit is given to the de-fuzzification unit which converts the linguistic variables into the numeric data in the crisp form.

9.4 Results of SEIG by ANFIS based STATCOM

The performance of SEIG by ANFIS controller based STATCOM is shown in Fig. 19. The harmonic spectrum of voltage is shown in Fig. 21. In the previous case the STATCOM is controlled by PI controller which is replaced here by ANFIS controller. The ANFIS controller operation is implemented by gauss method. The voltage error between the reference and estimated signals for ANFIS controller are become 2.3228e-06 which is very less. The output voltage of SEIG is also become constant at 400 V and the current is also balanced. The rotor speed and electromagnetic torque fluctuations are also become less.

9.5 Results of DFIG by ANFIS based DTC

ANFIS controller is implemented in direct torque control of DFIG to control the torque, speed, flux, current and voltage of the DFIG machine. The control model is similar to the model explained in previous section. The only difference is that the PI controller is replaced by the ANFIS controller. The results obtained from the DTC with PI controller are trained by using ANFIS editor and result is exported to the ANFIS controller. The results for the DTC using ANFIS controller are presented in Fig. 22.

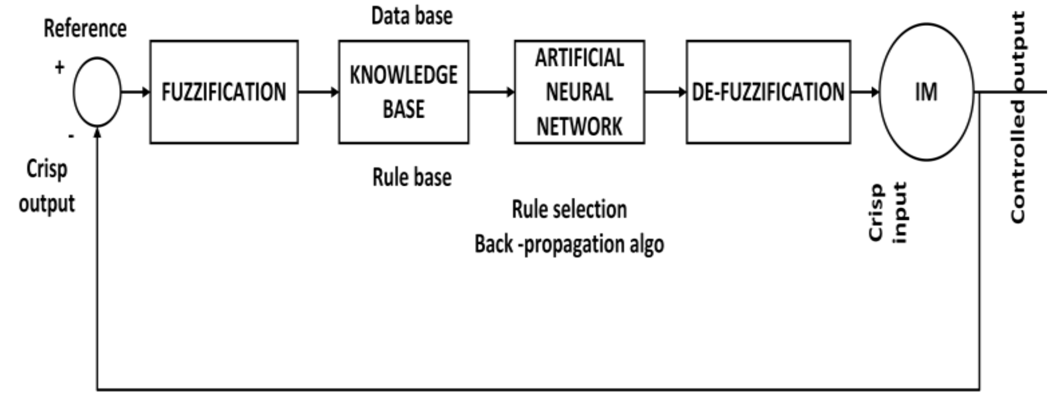

Fig. 18 Block diagram of ANFIS control scheme

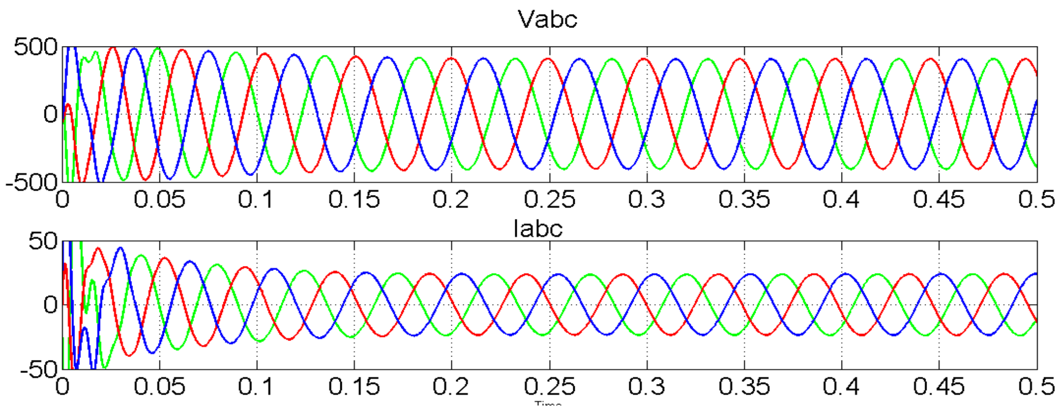

Fig. 19 SEIG voltage and current by ANFIS based STATCOM controller

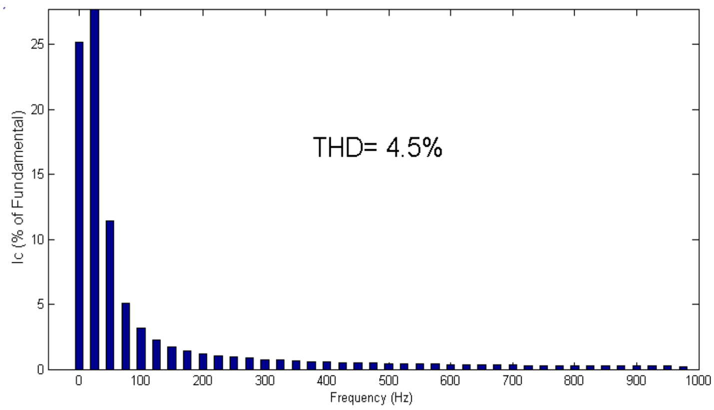

Fig. 20 Harmonic Spectrum of SEIG voltage when controlled by ANFIS based STATCOM

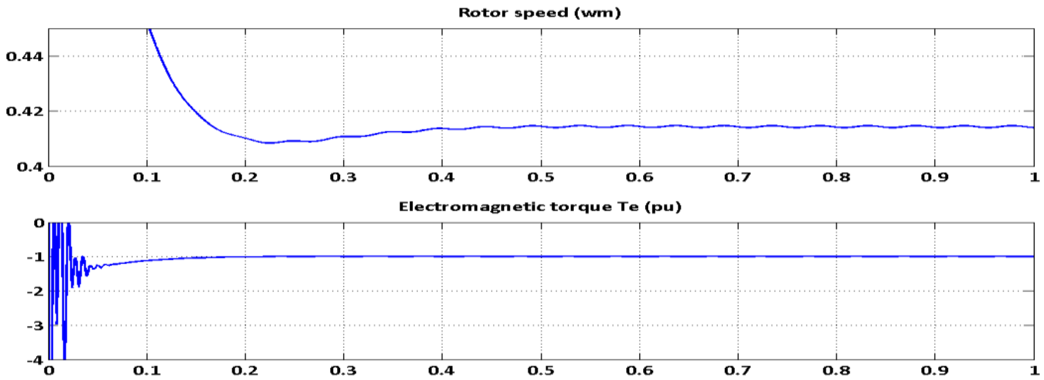

Fig. 21 ANFIS controlled SEIG-STATCOMRotor speed and Electromagnetic torque

Table 3 SEIG control strategies qualitative performance comparison

Controlling Scheme	ELC	STATCOM Controller	ANFIS Based STATCOM Regulator
Output Terminal Voltage (V)	200	400	400
Output Terminal Current (A)	45	25	25
Rotor Speed (pu)	0.3-0.4	0.414-0.415	0.4
Electromagnetic Torque (pu)	0-3	1	1
THD	15.86%	8%	4.5%
Voltage Regulation	poor	high	high
Settling time	high	low	low
Ripples	high	medium	less as compare to ELC and STATCOM controller
Computational complexity	very complex	very complex	less complex

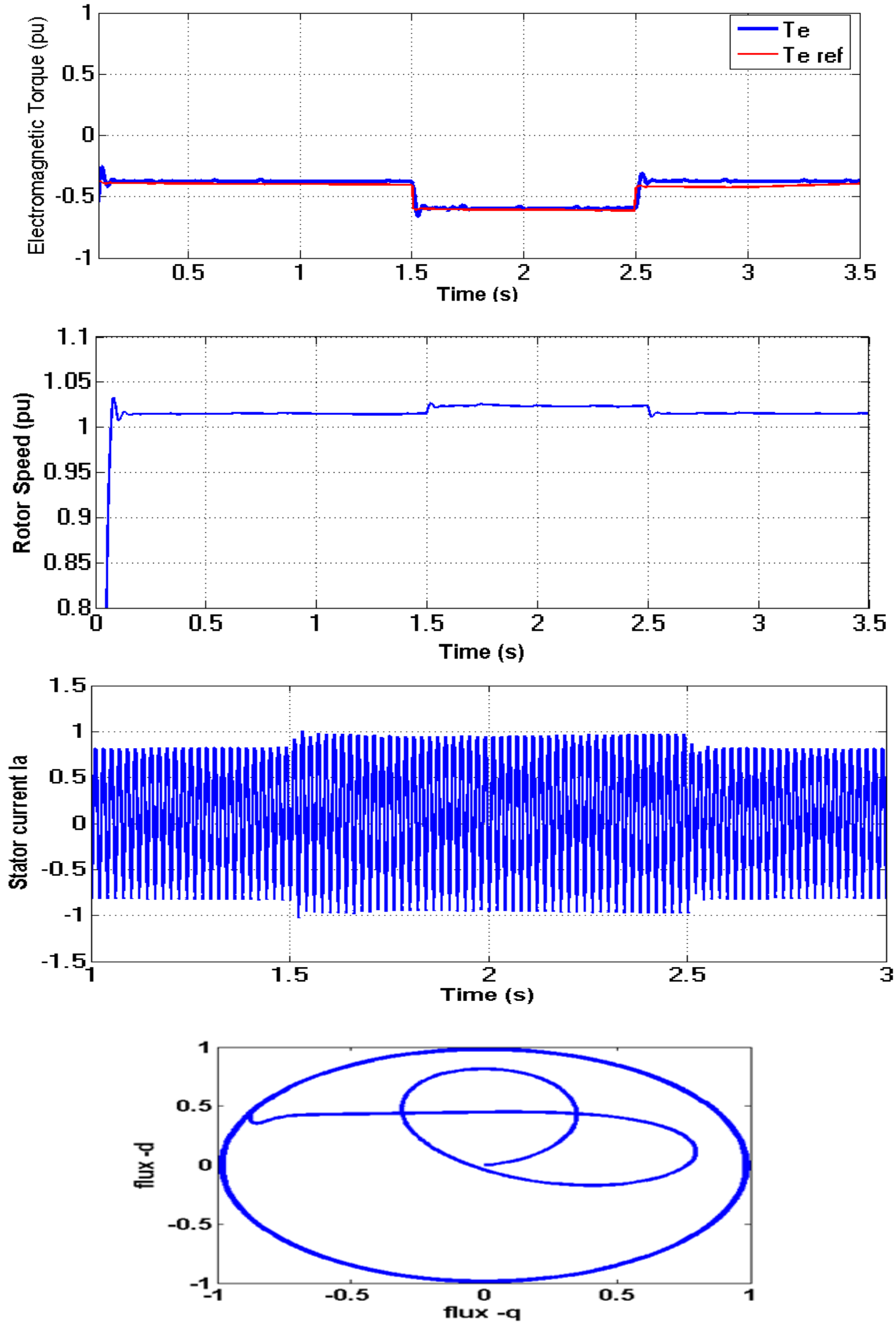

Fig. 22 Simulation result of DTC of DFIG using ANFIS controller

Table 4 DFIG control strategies qualitative performance comparison

Performance criterion	VC	DTC	DPC	ANFIS
Computational complexity	High	High	Low	Low
Machine model dependency	High	High	Low	Low
Transitory response	Medium	Medium	High	High
Settling time	Medium	Low	Low	Low
Peak overshoot	High	High	High	Low
Robustness	High	Medium	High	High
Ripples	High	Medium	Medium	Low
Overall implementation complexity	High	High	Medium	High

10. Conclusions

In this paper two types of induction generators namely SEIG and DFIG with different control techniques are compared. The voltage regulation performance of SEIG using ELC, STATCOM and ANFIS based STATCOM are analyzed, where the performance is poor for ELC and the system is complex. The voltage regulation of SEIG with STATCOM controller is much better than ELC (for STATCOM it gives 400 V and in cases of ELC it is only 200 V). The electromagnetic torque is also rated for STATCOM based controller and the total harmonic distortion (THD) level is also decrease from the level of 15.86% to 8%. But due to complexity of PI controller design and its performance at some operating conditions also need to be improved when fed to three phase load. Implementation of ANFIS based controller in STATCOM yields better voltage regulation and easy to design. Similarly for DFIG three control methods i.e. VC, DTC and DPC were implemented, these methods showed remarkable performance at steady state and transitory responses. The performance of DFIG using VC strategy imposes lower instrumentation constraints but its transient response is sluggish compared to the direct methods. DPC is less dependent on machine model as compared to VC and DTC method. While it is difficult to unmistakably assess whether DPC or DTC is better as control strategy for DFIG-based WECSs, it is clear from simulation results that the DTC strategy outperformed by the other two strategies but it is acknowledged that DTC is complex. All these three strategies have large peak overshoot and ripples, highest in the VC method. Further by replacing PI controller with ANFIS controller improves the performance of DTC. The reported results are likely to qualitatively hold for a wide range for both SEIG and DFIG-based WECS.

References

Alghuwainem, S.M. (1999), “Steady state analysis of an isolated self excited induction generator driven by regulated and unregulated turbine”, *IEEE T. Energy Conver.*, **14**(3), 718-723.

Alnasir, Z.A. and Almarhoon, A.H. (2012), “Design of direct torque controller of induction motor (DTC)”, *Int. J. Eng. Technol.*, **4**(2), May.

Aware, M.V., Kothari, A.G. and Choube, S.O. (2000), “Application of adaptive Neuro Fuzzy controller (ANFIS) for voltage source inverter fed induction motor drive”, *Proceedings of the 3rd International*

Proceedings of Power Electronics and Motion Control Conference (IPEMC 2000), August.
Bhim Singh, Senior Member, IEEE, S.S. Murthy, Life Senior Member, IEEE, and Sushma Gupta (2005), "Transient Analysis of Self-Excited Induction Generator with Electronic Load Controller (ELC) Supplying Static and Dynamic Loads", *IEEE Trans. On Industry Applications*, **41**(5), Sep/Oct.
Bhim Singh, Senior Member, IEEE, S.S. Murthy, Life Senior Member, IEEE, and Sushma Gupta (2006), "Analysis and design of electronic load controller for self-excited induction generators", *IEEE T. Energy Conver.*, **21**(1), March.
Bhim Singh, Senior Member, IEEE, S.S. Murthy, Life Senior Member, IEEE, and RajaShekhara Reddy Chilipi (2014), "STATCOM-Based Controller for a three phase SEIG Feeding Single Phase Load", *IEEE T. Energy Conver.*, **29**(2), June.
Bonert, R. and Hoops, G. (1989), "Stand alone induction generator with terminal impedance controller and no turbine controls", *Proc. IEEE Power Engineering Soc. Summer Meeting*, 28-31.
ChitraVenugopal University of Kwazulu Natal/School of Electrical, Electronics and Computer Engineering, South Africa (2010), "ANFIS Based Field Oriented Control for Matrix Converter fed Induction Motor" *2010 IEEE International Conference on Power and Energy (PECon2010)*, Kuala Lumpur, Malaysia, Nov 29 - Dec 1.
Datta, R. and Ranganathan, V.T. (2001), "Direct power control of grid-connected wound rotor induction machine without rotor position sensors", *IEEE T. Power Electr*., **16**(3), 390-399.
Global wind report (2015), http://www.gwec.net
Guo, J., Cai, X. and Gong, Y. (2008), "Decoupled control of active and reactive power for a grid-connected doubly-fed induction generator", *Proceedings of the 3rd International Conference on Electric Utility Deregulation and Restructuring and Power Technologies*.
Habetler, T., Profumo, F., Pastorelli, M. and Tolbert, L. (1992), "Direct torque control of induction machines using space vector modulation", *IEEE T. Ind. Applicat*., **28**(5), 1045-1053.
Henderson (1998), "An advanced electronic load governor for control of micro hydroelectric generation", *IEEE T. Energy Conver*., **13**(3), 300-304.
Jacomini, R.V., Rocha, C.M., Altuna, J.A.T. and Acue, J.L. (2014), "Implementation of a Neuro-Fuzzy direct torque and reactive power control for DFIM", *Proceedings of the IEEE 40th Conference of Industrial Electronics Society (IECON 2014)*, October.
Kusagur, A., Kodad, S.F. and Sankar Ram, B.V. (2010), "Modeling, design & simulation of an Adaptive Neuro Fuzzy Inference System (ANFIS) for speed control of induction motor", *Int. J. Comput. Appl.*, **vol.6**, no.12, pp.29-44, September.
Makky, M. and El-Latif, N.A. (1997), "Integral-cycle control with a d.c. chopper controller for single-phase induction motor", *Electr. Pow. Syst. Res*., **40**, 91-98.
Mechernene, A., Zerikat , M. and Chekroun, S. (2010), "Indirect field oriented adaptive control of induction motor based on Neuro-Fuzzy controller", *Proceedings of the 18th Mediterranean Conference on Control & Automation* Marrakech, Morocco ,June 23-25.
Moghadasia, M., Kiani, R., Betin, F., Lanfranchi, V., Yazidi, A. and Capolino, G.A., Department of Electrical Engineering, ShahidChamran, University, Ahvaz, Iran (2011), "Intelligent sensorless speed control of six-phase induction machine" , *978-1-61284-972-0/11/$26.00 © 2011 IEEE*.
Murthy, S.S., Singh, B., Gupta, S. and Gulati, B.M. (2003), "General steady state analysis of three-phase self-excited induction generator feeding three phase unbalanced load/single-phase load for stand-alone applications", *Proc. Inst. Elect. Eng., Gen., Transm. Distrib.*, **150**(1), 49-55.
Noguchi, T., Tomiki, H., Kondo, S. and Takahashi, I. (1998), "Direct power control of PWM converter without power-source voltage sensors", *IEEE T. Ind. Applicat.*, **34**(3), 473-479.
Nunes, M., Lopes, J. and Zurn, H. (2004), "Influence of the variable-speed wind generators in transient stability margin of the conventional generators integrated in electrical grids", *IEEE T. Energy Conver.*, **19**(4), 692-701.
Pingle, T., Patil, S. and Chopde, S. (2015), "Modeling and vector control of DFIG using multilevel inverter", *Int. Conference on Advancement in Power and Energy*, 222-227.

Qiao, W. (2009), "Dynamic modeling and control of doubly fed induction generators driven by wind turbines", *Proceedings of the Power Systems Conference and Exposition, 2009 IEEE/PES*, March.

Rajakaruna, S. and Bonert, R. (1993), "A technique for the steady-state analysis of a self-excited induction generator with variable speed", *IEEE T. Energy Convers*., **8**(4), 757-761.

Smith, N.P.A. (1996), "Induction generators for stand-alone micro-hydro systems", *Proceedings of the IEEE Int. Conf. Power Electronics Drive Energy Systems for Industrial Growth*, New Delhi, India.

Suarez, E. and Bortolotto, G. (1999), "Voltage-frequency control of a self-excited induction generator", *IEEE T. Energy Conver*., **14**(3), 394-401.

Sudhakar, A. and Vijaya Kumar, M. (2012), "A comparative analysis of PI and Neuro-Fuzzy controllers in direct torque control of induction motor drives", *Int. J. Eng. Res. Appl.*, **2**(4), 672-680.

Tremblay, E., Atayde, S. and Chandra, A. (2009), "Direct power control of a DFIG-based WECS with active filter capabilities", *Proceedings of the* 2009*IEEEElectrical Power Energy Conf. (EPEC 2009),* Montreal, QC, Canada, Oct. 22-23.

Tremblay, E., Atayde, S. and Chandra, A. (2011), "Comparative study of control strategies for the doubly fed induction generator in wind energy conversion systems: A DSP-based implementation approach", *IEEE T. Sustainable Energy*, **2**, 288-299.

Tremblay, E., Chandra, A. and Lagace, P. (2006), "Grid-side converter control of DFIG wind turbines to enhance power quality of distribution network", *Proceedings of the 2006 IEEE Power Engineering Society General Meeting (PES2006)*, Montreal, QC, Canada, Jun. 18-22.

Zarean, N. and Kazemi, H. (2012), "A new DTC control method of doubly fed induction generator for wind turbines", *Renew. energy and distributed generation*, 69-74.

Zhi, D. and Xu, L. (2007), "Direct power control of DFIG with constant switching frequency and improved transient performance", *IEEE T. Energy Conver*., **22**(1), 110-118.

CC

APPENDIX 1

System Parameters

1) *SEIG machine parameters:*
7.5 KW, 400V, 50 Hz, 4 pole, 1440 rpm. Y-connected
R_s= 0.03461 pu,
L_{ls}=0.04484 pu,
R_r= 0.0347pu,
L_{lr}= 0.04484 pu,
L_m=1.827 pu
Inertia constant (J) = 0.05642.

2) *Electronic load controller parameters:*
Rectifier parameters:
Input resistance = 1 Ω,
Input inductance = 1 mH,
DC filtering capacitor =4000 μF,
Dump load resistance = 120 Ω,
PI controller: $K_p = 100,\ K_i = 100,$

3) *STATCOM parameters:*
Three leg IGBT VSI:
Input inductance = 50 H,
DC capacitance =100 μF,
PI controller:$K_p = 10,\ K_i = 5,$

APPENDIX 2

1) *DFIG machine parameters:*
2 MVA, 690 V (L-L), 50 Hz, 4 pole
R_s= 0.03513pu,
L_{ls}= 0.04586pu,
R_r= 0.03488pu,
L_{lr}= 0.04586pu,
L_m=1.352pu

Nomenclature

[R]	SEIG resistance
[L]	SEIG inductance
[G]	Speed inductance
P	Number of poles
n_p	Number of pole pairs
ω_r, ω_{slip}	Rotor electrical speed and slip speed
T_{shaft}	Input torque
T_e	Electromagnetic torque
I_m	Magnetizing current
L_m	Magnetizing inductance
a, b, c, d	Coefficient of magnetizing curve
V_s, V_r	Stator and rotor Voltage
i_s, i_r	Stator and rotor current
J	Inertia constant
w_g	Angular speed
L_s, L_r	Stator and rotor self-inductance
L_m	Mutual inductance
I_l	Load current
$\overline{I_{ld}}$	Fundamental component of d-axis load current
$\widetilde{I_{ld}}$	Oscillatory component of d-axis load current
$\overline{I_{lq}}$	Fundamental component of q-axis load current
$\widetilde{I_{lq}}$	Oscillatory component of q-axis load current
V_{dc}	Dc-bus capacitor voltage
V_t	SEIG terminal voltages
V_a, V_b, V_c	Three phase SEIG terminal voltage
I_{pi}	Output of the PI controller
I_D	Resultant d-axis component of current
I_Q	Resultant q-axis component of current
ϕ_s, ϕ_r	Stator and rotor flux
σ	Leakage coefficient
Ps, Qs	Stator active and reactive power